Antifungal Behavior of Silicon-incorporated Diamond-like Carbon by Tuning Surface Hydrophobicity with Plasma Treatment

Kai-Hung Yang[1], Parand Riley[1], Keith B. Rodenhausen[2], Shelby A. Skoog[3], Shane J. Stafslien[5], Lyndsi Vanderwal[5], Roger J, Narayan[1,4*]

1. Department of Materials Science and Engineering, NC State University, Raleigh, NC, 27695, USA
2. Anton Paar USA, Ashland, VA 23005, USA
3. Center for Devices and Radiological Health, U.S. Food and Drug Administration, Silver Spring, MD 20993, USA
4. UNC/NCSU Joint Department of Biomedical Engineering, Raleigh, NC 27695, USA
5. Department of Coatings & Polymeric Materials, North Dakota State University, 58102, USA

Corresponding author: rjnaraya@ncsu.edu

Abstract

Silicon-incorporated diamond-like carbon (DLC), an amorphous material containing Si atoms with sp^3 and sp^2 hybridized carbon, is a promising biomaterial for versatile biomedical applications due to its excellent mechanical properties, chemical inertness, biocompatibility, and antimicrobial capability. However, the antifungal properties of plasma-treated Si-DLC have not been systematically evaluated. In this study, Si-DLC coatings were deposited by chemical vapor deposition and further treated with either oxygen or fluorine plasma to render the surface anchored with different functional groups and hydrophobicity. Surface roughness was probed with atomic force microscopy (AFM), while bonding character and surface composition were assessed using Raman and X-ray photoelectron spectroscopy (XPS). Wettability and surface charge were investigated via water contact angle and zeta potential measurements. Antifungal assessment was performed using a *Candida albicans* multi-well plate screening technique and crystal violet biomass quantification. The results demonstrate that oxygen plasma treated Si-DLC exhibited hydrophilic properties, lower negative zeta potential, and significant antifungal behavior. This material can potentially be applied on surfaces for the prevention of reduced nosocomial infections.

Keywords: zeta potential, hydrophobicity, antifungal, diamond-like carbon, plasma treatment

Introduction

Carbon-based materials have been used in numerous fields of research, including biomaterials[1,2] because of their abundance, accessibility, and exceptional properties. Among these materials, diamond-like carbon (DLC), an amorphous material composed of sp^3 and sp^2 hybridized carbon[3], has been widely studied for biomedical devices to extend the lifespan of implants and to improve the efficacy of regenerative treatments[4, 5]. The excellent mechanical and tribological properties[6], chemical inertness[7], biocompatibility[8], and antimicrobial capability[9] of DLC are ideal for medical instrumentation and implantable devices, such as medical wire and needles[10], blood pumps[11], heart valves[12], and joint prostheses [13]. Additionally, the relatively low deposition temperature compared with deposition of crystalline diamond make DLC suitable for various substrate materials.

Several thin film coating techniques have been applied for the deposition of DLC, including both chemical vapor deposition (CVD) and physical vapor deposition (PVD). Moreover, Gotzmann *et al.* have demonstrated that the DLC coatings deposited by these techniques all exhibit biocompatible properties[14]. In recent years, plasma enhanced CVD (PECVD) has been widely applied for the deposition of DLC[5,8,15] with reasonable deposition rate, coating uniformity, and suitability for large-scale manufacturing[16]. To prevent the delamination of the DLC coating from the substrate and subsequent failure of a medical device, silicon incorporation into DLC has been shown to reduce the internal stress of the film and to promote better adhesion of DLC with the substrate[17]. Additionally, Wu and Hon [18] demonstrated improved thermal stability of DLC films by the addition of silicon; Kim et al. showed that a low friction coefficient was observed with silicon-incorporated DLC[19]. These findings, coupled with the aforementioned properties of DLC, enhance the potential for this carbon-based material in biomedical applications.

Despite these favorable properties, one critical factor in considering the practical use of DLC in biomedical devices is the potential inhibition of microorganisms. The initial attachment of bacteria or fungus leads to biofilm formation, which protects the microorganisms from phagocytosis and provides resistance to antimicrobial treatment [5,20]. The high incidence of infections resulting from the use of implanted biomedical devices jeopardizes patient health and increases health care costs [21]. The removal or replacement of the medical device is often suggested once the infection is diagnosed in order to avoid further severe and potentially lethal complications. However, removal or

replacement procedures include various risks and have the potential to further expose the patient to increased risk of infection.

In a nationwide surveillance study, *Candida* species were identified as the fourth leading cause of nosocomial bloodstream infections in the United States, accounting for 8% of all bloodstream infections, and were associated with up to 40% patient mortality[22,23]. Among *Candida* species, *Candida albicans* was the most commonly found fungal pathogen, although it was also found as commensal fungus in the gastrointestinal tract and oral cavity[5]. In previous studies, the dependence of antimicrobial properties on the surface hydrophobicity of carbon-based materials was reported[9]. However, the antifungal properties of plasma-treated Si-DLC have not been evaluated. In this study, the goal was to investigate the influence of different surface termination and hydrophobicity of Si-DLC coatings on antifungal properties. Plasma surface treatment was conducted after Si-DLC deposition to render the surface either terminated with oxygen-containing species or fluorine-containing species. Exposing Si-DLC to oxygen plasma is known to render the surface highly hydrophilic [8]. Concurrently, the plasma treatment may result in selective etching and cause a change in surface morphology. Therefore, surface roughness was measured with AFM while Raman and XPS were applied to investigate the resulting composition and bonding character of the coating. Wettability and surface charge were investigated via water contact angle and zeta potential measurements while antifungal behavior was assessed using *Candida albicans* and crystal violet staining.

Materials and methods

Silicon-incorporated diamond-like carbon (Si-DLC) deposition

A custom-designed radio frequency (RF) plasma-enhanced chemical vapor deposition (PECVD) system located in the Nanofabrication Facility (NNF) at North Carolina State University (NCSU) was utilized for silicon-incorporated diamond-like carbon (Si-DLC) deposition on Si (100) substrates and aluminum disks. The PECVD system was designed to generate plasma in capacitively coupled mode. Inside the stainless-steel cylindrical chamber, a driving electrode with a diameter of approximately 12 inches was placed on the bottom of the chamber as the substrate holder while the driving electrode was electrically insulated from the chamber body. The rest of the chamber acted as the counter electrode and was grounded as shown in Figure 1. The plasma was generated by an RFX-600 radiofrequency (RF) power supply (Advanced Energy Industries, Inc., Denver, CO, USA) with a 13.56 MHz

frequency. The pumping system provided a base pressure of approximately 1.6 x 10^{-8} Torr. The argon, oxygen, and tetramethylsilane (TMS) process gases flowed into the chamber from the gas inlet at the top of the chamber through a showerhead distribution ring. The deposition procedure consisted of loading, plasma cleaning, plasma deposition, and unloading steps. Following loading and an overnight pump-down procedure, the plasma cleaning step was conducted for 10 min by argon and oxygen gases with a mass flow rate of 90 standard cubic centimeters per minute (sccm) and 50 sccm, respectively. During the cleaning step, the peak-to-peak voltage (V_{pp}) was kept at 400 ± 10 V with an RF power of 84 ± 10 W and a DC bias of -153 ± 10 V. The Si-DLC deposition was carried out by using 1.6 sccm of TMS and 90 sccm of argon with 50 min duration, a V_{pp} of 200 ± 10 V, an RF power of 57 ± 10 W, and a DC bias of -72 ± 10 V. The working pressure was kept at 50 mTorr using a Baratron® pressure gauge (MKS Instruments, Inc., Andover, MA, USA) during the cleaning and the deposition steps. The deposition rate of Si-DLC was calculated to be ~6 nm/min.

Surface termination by plasma treatment

Tailored surface properties of Si-DLC can be achieved by plasma treatment to terminate the surface with oxygen-containing species or fluorine-containing species, resulting in different degrees of hydrophilicity. Plasma treatment was performed using a Plasmalab80Plus reactive ion etcher (RIE) (Oxford Instruments Plasma Technology, Concord, MA, USA) to render the surface oxygen or fluorine terminated. A gas flow of 50 sccm O_2 with a working pressure of 35 mTorr and a power of 100 W were applied for a duration of 20 s for oxygen plasma treatment. For fluorine plasma treatment, a gas flow of 25 sccm Ar and 25 sccm CHF_3, a working pressure of 35 mTorr, power of 50 W, and duration of 30 s were applied. The power and duration were optimized to minimize the etching of the DLC coating.

Surface roughness

The surface roughness of the DLC coatings was measured by atomic force microscopy (AFM) using an MFP-3D-BIO AFM (Oxford Instruments Asylum Research, Santa Barbara, CA, USA) to investigate the change in surface roughness before and after plasma treatment. The resulting AFM images based on 5 μm x 5 μm scans were obtained using tapping mode at a 300 kHz resonant frequency under ambient conditions.

Structure characterization

For structural characterization and investigation of sp hybridization, an alpha300 Raman spectroscopy imaging system (WITec Wissenschaftliche Instrumente und Technologie GmbH, Ulm, Germany) was employed to characterize Si-DLC coated samples. The Raman spectroscopy instrumentation was equipped with a solid-state green laser (532 nm) and a UHTS 300 spectrometer for signal detection. Raman spectra were acquired using a laser spot size of approximately 2 μm diameter and calibrated by the characteristic peak of Si (100) at 520.6 cm^{-1} with a resolution of 1 cm^{-1}.

Surface composition

A FlexMod X-ray photoelectron spectroscopy (XPS) system (SPECS Surface Nano Analysis GmbH, Berlin, Germany) was applied to characterize the surface chemistry to confirm the grafting of functional groups. Signals were collected using Mg kα excitation (1254 eV) and PHOIBIS 150 hemispherical electron analyzer (SPECS Surface Nano Analysis GmbH, Berlin, Germany) with takeoff angle at normal to surface X-ray incidence angle of 30° and X-ray source to analyzer angle of 60°. The analysis chamber exhibited a base pressure in the 10^{-10} mbar range. Energy calibration was determined by referencing the data to that of adventitious carbon. Compositional analysis of the spectrum and deconvolution were conducted with CasaXPS software (Casa Software Ltd., United Kingdom) using the Voigt function (Gaussian/Lorentzian) for line shape fitting.

Wettability

The hydrophilicity of the Si-DLC coatings was characterized by optical contact angle measurements using an OCA 200 contact angle goniometer and drop shape analysis system (DataPhysics Instruments USA Corp., Charlotte, NC, USA). Images were captured 5 s after adding a 0.2 μL distilled water droplet; contact angle measurements were determined using ellipse fitting of the droplet profile. Ten measurements for each sample type were analyzed for water contact angle.

Zeta potential

The zeta potential of the DLC coatings was measured using a SurPASS 3 Electrokinetic Analyzer (Anton-Paar GmbH, Graz, Austria). For each sample type, two rectangular pieces were cut and loaded into the instrument's adjustable gap cell. The sample surfaces faced each other to form a streaming channel with a separation distance of

approximately 100 μm. The streaming potential was assessed as a function of the pressure drop across the sample cell during the measurement. Then the zeta potential ζ was determined by the Helmholtz-Smoluchowski equation:

$$\zeta = \frac{\mathrm{d}U}{\mathrm{d}P}\frac{\eta}{\varepsilon_{\mathrm{r}}\varepsilon_0}k_{\mathrm{B}}$$

where $\mathrm{d}U$ is the differential streaming potential, $\mathrm{d}P$ is the differential pressure drop, η is the solution viscosity, ε_{r} is the solution relative permittivity, ε_0 is the vacuum permittivity and k_B is the electrolyte conductivity [24,25]. The sample surfaces were probed using 1 mM KCl with the addition of 0.05 M KOH solution or 0.05 mM HCl solution to increase or decrease the pH value. During the rinse cycle, 100 mL of electrolyte solution were withdrawn by the instrument and pressurized to 600 mbar. Then the electrolyte solution was released through the streaming channel and recovered. The sample surfaces were exposed to three rinse cycles of the probing solution for equilibration; the surfaces were exposed to three additional rinse cycles, during which streaming potential was measured as a function of the drop in pressure across the sample cell.

Antifungal evaluation

The antifungal behavior of DLC coatings was evaluated by crystal violet quantification after exposure to the opportunistic fungal pathogen *Candida albicans*. Prior to biofilm quantification, *Candida albicans* was incubated in 1× Yeast nitrogen base (YNB) + 100 mM dextrose overnight and was re-suspended in 1:10 RPMI 1640 medium/deionized water to a density of 10^7–10^8 cells/mL. Samples were seeded with 1 mL of the cell suspension and incubated at 37 °C for 24 h to promote cell attachment and growth. The samples were rinsed 3 times with PBS, dried at ambient conditions for 1 h, and then stained with 0.5 mL of 0.35% crystal violet dye solution (in DI water) for 15 min. Excess crystal violet solution was removed with further rinsing 3 times in DI water and drying for 1 h. Five hundred microliters of 33% glacial acetic acid were then applied to solubilize crystal violet dye bound to retained *Candida albicans*. After 15 min, a 150 μL aliquot of acetic acid extract was transferred to a 96-well plate; the absorbance was measured at a wavelength of 600 nm using a multi-well microplate spectrophotometer. Four replicates of each sample were performed. Background absorbance of the control samples (growth media without fungi) were subtracted from each respective sample.

Results and Discussion

Surface modification of DLC coatings using plasma treatment may be applied to tailor surface properties for specific biomedical applications; however, it is important to understand the impact of the surface modifications on the resulting surface properties (e.g., surface morphology, bonding character, surface composition, wettability and surface charge), as these characteristics may impact coating performance and biological interactions. Therefore, in this study, the effects of surface functionalization of DLC on various physical-chemical properties as well as the impact on antifungal characteristics were evaluated.

Three types of DLC coatings, Si-DLC, O-Si-DLC, and F-Si-DLC, were subject to AFM measurements for probing the change in surface roughness after plasma treatment. The resulting AFM images are shown in Figure 2; the root-mean-square (RMS) values of the surface roughness were 433 pm (Si-DLC), 402 pm (O-Si-DLC), and 448 pm (F-Si-DLC), respectively. The slight change in roughness between the unmodified Si-DLC and plasma-treated DLC was attributed to plasma-induced etching of Si-DLC, as oxygen plasma is known to remove carbon atoms easily[26]. However, this roughness change was minor due to the minimized plasma treatment duration. The results supported the similarity in surface roughness/morphology of the three samples.

The Raman spectra for the structural analysis of the DLC coatings on silicon substrates are depicted in Figure 3. The Raman spectrum of DLC is composed of two bands, one at about 1580 cm^{-1} (G peak) and the other at approximately 1350 cm^{-1} (D peak)[27, 28]. Typically, the D and G peaks of silicon-incorporated DLC show a redshift in wavelength in comparison to DLC[29]. The G peak originated from the in-plane vibrational mode of sp^2 hybridized carbon (Brillouin zone center phonons of E_{2g} symmetry). The D peak was assigned to the breathing of A_{1g} mode[30,31]. The spectra of the three samples were acquired in the range of 800-2000 cm^{-1}. The Gaussian distribution method was utilized for the deconvolution of the spectrum and fitting of the D and G peaks. The D and G peaks of the Si-DLC film were determined to be at 1339 cm^{-1} and 1482 cm^{-1}, respectively. The G peaks of O Si-DLC and F Si-DLC were located at 1498 cm^{-1} and 1493 cm^{-1} with the D peaks of 1360 cm^{-1} and 1353 cm^{-1}, respectively. Thus, all three spectra confirmed the presence of DLC structure on the silicon substrate. The intensity ratio of the two peaks (I_D/I_G) was directly related to the sp^2/sp^3 ratio and has been widely used for the qualitative estimation of the changes in the sp^2/sp^3 ratio[32–34]. With the incorporation of the oxygen and fluorine atoms on the surface of the Si-DLC coatings, the G peak position shifted to higher wavenumber values, from 1482 cm^{-1} of untreated Si-DLC to 1498 cm^{-1} and 1493 cm^{-1}, respectively. At the same time, the I_D/I_G ratio increased from 0.27 to

0.71 and 0.72 for O-Si-DLC and F-Si-DLC. This is indicative of an increase in sp^2/sp^3 ratio on the surface of O-Si-DLC and F-Si-DLC films and formation of small sp^2 clusters on the surface, since the olefinic sp^2 bonds are shorter than aromatic bonds which exhibit higher vibrational frequencies.

XPS was applied to characterize the grafting of functional groups on the coating surface. The results of XPS measurement before and after plasma treatment are shown in Figure 4; Table I summarizes the elemental composition of each DLC coating. The spectra demonstrated that the plasma treatments were successful by the presence of the predominant oxygen and fluorine features with respect to untreated Si-DLC. The atomic ratio of oxygen reached 54% on the surface of the oxygen plasma-treated Si-DLC compared to 10% on unmodified Si-DLC. As compared with evaluation of plasma surface modification of nitrogen incorporated ultrananocrystalline diamond (N-UNCD) in our previous study[35], Si-DLC samples exhibit a higher susceptibility for anchoring oxygen termination as only 16.2% of oxygen was observed on oxygen-terminated N-UNCD. However, the atomic ratio of fluorine for F-Si-DLC was similar to that fluorine-terminated N-UNCD. To further understand the bonding character on the surface, deconvolution of C 1s region for all the Si-DLC are shown in Figure 4(d-f) with the percentage of contribution listed in Table II. In Si-DLC, peaks centered at 283.3 eV, 284.3 eV, 285.1 eV, and 287.3 eV were observed, which corresponded to Si-C, sp^2, sp^3, and C=O bonding, respectively. In O-Si-DLC, an additional peak centered at 286.8 eV was visible, which indicated that C-O bonding was introduced by the oxygen plasma treatment. As for F-Si-DLC, four additional peaks located at 286.5eV, 288.8 eV, 290.5 eV, and 292.8 eV were identified, which corresponded to C-CF, C-F, C-F_2, and C-F_3 bonding, respectively. Both plasma treatments reduced the coverage of carbon on the surface by introducing oxygen or fluorine; the sp^3 carbon content decreased more significantly than the sp^2 carbon content. Preferential etching of sp^2 carbon over sp^3 carbon by oxygen plasma has been reported in the literature due to the lower activation energy of oxidation [36]. It was hypothesized that more sp^3 carbon was subjected to bond breaking and anchoring of functional groups since sp^2 carbon was removed from the surface by the formation of CO and CO_2.

The water contact angle optical images are shown in Figure 5(a-c), with measurements of 91.0 ± 0.7° for Si-DLC, 50.4 ± 1.4° for O-Si-DLC, and 81.0 ± 1.0° for F-Si-DLC, respectively. The results were obtained by averaging n=10 measurements. As shown, the unmodified Si-DLC is hydrophobic, which is partially due to the Si content. In a study

by Ahmed et al. [37], Si-doped DLC demonstrated higher water contact angle measurements compared with undoped DLC. Oxygen plasma treatment rendered the surface most hydrophilic by introducing polar C-O bonding as compared with Si-DLC. These results are consistent with those of our previous study[8]. In contrast, F-Si-DLC was still relatively hydrophobic[38,39], which may be due to the introduction of less densely packed fluorocarbon compared with hydrocarbon as demonstrated in the literature using atomistic molecular simulation [40] and reduced surface free energy, which echoed the results of the XPS measurements with 35% contribution of fluorocarbon in the C 1s peak. In this study, Si-DLC without plasma treatment was more hydrophobic than both O-Si-DLC and F-Si-DLC. In our previous study on N-UNCD, the unmodified N-UNCD was slightly more hydrophilic than F-terminated N-UNCD. These differences in coating wettability may be due to the stronger effects of Si-incorporation on hydrophobicity than the fluorine surface treatment or due to differences in surface roughness and/or degree of surface functionalization.

Since the Si-DLC samples are insulating with or without plasma treatment, streaming potential measurements were adopted to obtain the optimized zeta potential, which is independent of the surface area exposed to the electrolyte and not be affected by surface roughness. The resulting zeta potentials versus electrolyte solution pH value, ranging from 3 to 10, are shown in Figure 5(d). The curve was fitted with a sigmoid function. In acidic electrolyte solution (pH=3), the zeta potential of untreated Si-DLC (-9 mV) was less negative than the other two coatings, with O-Si-DLC the most negative (-23.8 mV) and F-Si-DLC in between (-16.8 mV). The extrapolated isoelectric points (IEP) were in the same sequence. When the electrolyte solution pH value was increased to basic pH 10, O-Si-DLC exhibited less negative zeta potential (-69.3 mV) than both untreated Si-DLC (-95.8 mV) and F-Si-DLC (-92.1 mV) coatings. The negative zeta potentials could indicate that electron transfer occurred from aqueous solution to Si-DLC or the presence of ionization of oxygen-containing groups on the surface[41]. Figure 5 demonstrates that the zeta potential of O-Si-DLC is less susceptible to electrolyte solution pH change, increasing by 45.5 mV with decreasing pH. In contrast, the zeta potential of untreated Si-DLC and F-Si-DLC varied with pH value more significantly, with increasing zeta potential by 86.8 mV and 75.3 mV, respectively, with decreasing pH. In a study of the correlation between the water contact angle and the zeta potential of low-density polystyrene, Temmel *et al.* suggested that the hydrophilic surface could lead to increased adsorption of water, resulting in a decrease in anion adsorption [42]. Therefore, for hydrophilic surfaces, a shift of zeta potential to less negative value was observed at

high pH values compared to hydrophobic surfaces. Using molecular dynamics simulations, Kudin and Car demonstrated that hydrophobic surfaces acquired a net negative charge by localized hydroxide ion in the surface layer[43], which further correlated the wettability with zeta potential. In our previous study, N-UNCD with a hydrophilic surface exhibited a less negative zeta potential while the hydrophobic surface exhibited more negative zeta potential at high pH values[35]. These studies are consistent with the observations in this study.

The results of antifungal assessment based on *Candida albicans* with crystal violet quantification are shown in Figure 6 with (a) the images and (b) absorbance measurements of the samples. The percentage of biofilm inhibition was calculated with respect to the polystyrene control as[44]:

% biofilm inhibition = [1 – (OD_{600} of samples with coating/OD_{600} of polystyrene control) × 100]

Among the three types of samples, O-Si-DLC demonstrated the highest percent inhibition with 99.5%; the inhibitions were 22.8% and 24% for F-Si-DLC and Si-DLC, respectively. These results indicate that a hydrophilic surface has higher percent inhibition for biofilm growth. It has been well studied that the adhesion of *Candida albicans* depends on the *van der Waals* and hydrophobic interactions[45]. The solid surface with hydrophobic character could facilitate the attachment of *Candida albicans* and, thus, less antifungal characteristics. Moreover, the repelling of water by the hydrophobic surface could further bring the cells close to the liquid-solid interface[46], which can serve as another benefit for the attachment of cells. The hydrophobicity due to the incorporation of silicon in DLC [15] may be attributed to the low percent inhibition of *Candida albicans* on unmodified Si-DLC observed in this study. Similarly, the less densely packed fluorocarbons resulted in a low surface free energy and hydrophobicity[40] for the F-Si-DLC, which led to low percent inhibition of *Candida albicans* attachment and growth. Although Zhao *et al.* have demonstrated that the incorporation of silicon in DLC resulted in an increase in sp^3/sp^2 ratio and decrease in bacterial adhesion[47], the case may differ from one microbial species to another and may also depend on the other factors such as cell surface hydrophobicity[48].

Since a large number of nosocomial infections are attributed to adhesion and biofilm formation of *Candida albicans* on host tissues or implanted devices[46], evaluation of antifungal surface treatments to prevent and/or minimize potential infections associated with medical devices is of significant interest. Si-DLC films have potential as implant coatings. The surface chemistry can be easily adjusted by plasma treatment, which enables tunable surface

properties for different medical applications. Detailed investigation of pathogen and solid interface interactions should be performed prior to the use of these coatings in medical applications.

Conclusions

In this work, Si-DLC containing 19% Si was deposited using a custom-designed PECVD system and further treated with oxygen and fluorine plasma to alter the surface chemistry and resulting hydrophobicity. Low surface roughness and no significant change in morphology after plasma treatment were observed. Successful surface termination and increased coverage of C-O and C-F bonding were confirmed with XPS providing distinct surface chemistry and, hence, different wettability. Water contact angle measurements correlated with the zeta potential of the surface at high pH values suggested by a mechanism of anion adsorption. The interaction of *Candida albicans* with the three different Si-DLC surfaces was evaluated by crystal violet quantification, showing more significant inhibition with hydrophilic O-Si-DLC surface; the hydrophobic nature of Si-DLC and F-Si-DLC resulted in more negative zeta potential and increased hydrophobic interactions with *Candida albicans*. Although the results suggested that a hydrophilic Si-DLC surface possesses better antifungal properties against *Candida albicans*, the results may differ between different microbial species. The properties of the surfaces and the microorganisms may affect the tendency for microbial attachment and biofilm growth. This study demonstrated that Si-DLC can serve as a platform with versatile surface hydrophobicity and zeta potential. The ability to tailor the surface chemistry and resulting properties imparts Si-DLC with great potential as a biomaterial for reducing nosocomial infection. Coatings applied to medical devices for antimicrobial effects will be investigated with other microbial species in future studies.

FDA Disclaimer

The findings and conclusions in this paper have not been formally disseminated by the Food and Drug Administration and should not be construed to represent any agency determination or policy. The mention of commercial products, their sources, or their use in connection with material reported herein is not to be construed as either an actual or implied endorsement of such products by the Department of Health and Human Services.

References

1. Al-Jumaili A, Alancherry S, Bazaka K, Jacob MV. Review on the antimicrobial properties of carbon nanostructures. Materials. 2017 Sep;10(9):1066.

2. Paul R. Diamond-like-carbon coatings for advanced biomedical applications. Glob. J. Nano. 2017;2(5):555598.

3. Ohgoe Y, Hirakuri KK, Saitoh H, Nakahigashi T, Ohtake N, Hirata A, Kanda K, Hiratsuka M, Fukui Y. Classification of DLC films in terms of biological response. Surface Coatings Technol. 2012 Aug 25;207:350-4.

4. Milan PB, Khamseh S, Zarrintaj P, Ramezanzadeh B, Badawi M, Morisset S, Vahabi H, Saeb MR, Mozafari M. Copper-enriched diamond-like carbon coatings promote regeneration at the bone–implant interface. Heliyon. 2020 Apr 1;6(4):e03798.

5. Akkam Y, Alshurman K. Fabricating ultra-smooth diamond-like carbon film and investigating its antifungal and antibiofilm activity. J. Biomim. Biomater. Biomed. Eng. 2019;43:109-123.

6. Hauert RJ. An overview on the tribological behavior of diamond-like carbon in technical and medical applications. Tribology Int. 2004 Nov 1;37(11-12):991-1003.

7. Sun CQ, Xie H, Zhang W, Ye H, Hing P. Preferential oxidation of diamond {111}. J. Phys. D. 2000 Sep 7;33(17):2196.

8. Movahed S, Nguyen AK, Goering PL, Skoog SA, Narayan RJ. Argon and oxygen plasma treatment increases hydrophilicity and reduces adhesion of silicon-incorporated diamond-like coatings. Biointerphases. 2020 Jul 31;15(4):041007.

9. Cumont A, Pitt AR, Lambert PA, Oggioni MR, Ye H. Properties, mechanism and applications of diamond as an antibacterial material. Funct. Diamond. 2021 Jan 2;1(1):1-28.

10. Dearnaley G, Arps JH. Biomedical applications of diamond-like carbon (DLC) coatings: A review. Surface Coatings Technol. 2005 Dec 21;200(7):2518-24.

11. Alanazi A, Nojiri C, Kido T, Noguchi J, Ohgoe Y, Matsuda T, Hirakuri K, Funakubo A, Sakai K, Fukui Y. Engineering analysis of diamond-like carbon coated polymeric materials for biomedical applications. Artif. Organs. 2000 Aug 1;24(8):624-7.

12. Tran HS, Puc MM, Hewitt CW, Soll DB, Marra SW, Simonetti VA, Cilley JH, DelRossi AJ. Diamond-like carbon coating and plasma or glow discharge treatment of mechanical heart valves. J. Invest. Surg. 1999 Jan 1;12(3):133-40.

13. Onate JI, Comin M, Braceras I, Garcia A, Viviente JL, Brizuela M, Garagorri N, Peris JL, Alava JI. Wear reduction effect on ultra-high-molecular-weight polyethylene by application of hard coatings and ion implantation on cobalt chromium alloy, as measured in a knee wear simulation machine. Surface Coatings Technol. 2001 Jul 1;142:1056-62.

14. Gotzmann G, Beckmann J, Wetzel C, Scholz B, Herrmann U, Neunzehn J. Electron-beam modification of DLC coatings for biomedical applications. Surface Coatings Technol. 2017 Feb 15;311:248-56.

15. Ahmed MH, Byrne JA, Ahmed W. Characteristic of silicon doped diamond like carbon thin films on surface properties and human serum albumin adsorption. Diamond Related Mater. 2015 May 1;55:108-16.

16. Luo JK, Fu YQ, Le HR, Williams JA, Spearing SM, Milne WI. Diamond and diamond-like carbon MEMS. J. Micromech. Microeng. 2007 Jun 28;17(7):S147.

17. Damasceno JC, Camargo Jr SS, Freire Jr FL, Carius R. Deposition of Si-DLC films with high hardness, low stress and high deposition rates. Surface Coatings Technol. 2000 Nov 1;133:247-52.

18. Wu WJ, Hon MH. Thermal stability of diamond-like carbon films with added silicon. Surface Coatings Technol. 1999 Jan 29;111(2-3):134-40.

19. Kim MG, Lee KR, Eun KY. Tribological behavior of silicon-incorporated diamond-like carbon films. Surface Coatings Technol. 1999 Feb 1;112(1-3):204-9.

20. Kaleli-Can G, Hortaç-İştar E, Özgüzar HF, Mutlu M, Mirza HC, Başustaoğlu A, Göçmen JS. Prevention of Candida biofilm formation over polystyrene by plasma polymerization technique. MRS Comm. 2020 Dec;10(4):667-73.

21. Zhao Q, Liu Y, Wang C, Wang S. Evaluation of bacterial adhesion on Si-doped diamond-like carbon films. Appl. Surf. Sci. 2007 Jun 30;253(17):7254-9.

22. Wisplinghoff H, Bischoff T, Tallent SM, Seifert H, Wenzel RP, Edmond MB. Nosocomial bloodstream infections in US hospitals: analysis of 24,179 cases from a prospective nationwide surveillance study. Clin. Infect. Dis. 2004 Aug 1;39(3):309-17.

23. Wenzel RP, Gennings C. Bloodstream infections due to Candida species in the intensive care unit: identifying especially high-risk patients to determine prevention strategies. Clin. Infect. Dis. 2005 Sep 15;41(Supplement_6):S389-93.

24. Luxbacher T. The Zeta Potential for Solid Surface Analysis: A practical guide to streaming potential measurement. Anton Paar GmbH; 2014.

25. Bukšek H, Luxbacher T, Petrinić I. Zeta potential determination of polymeric materials using two differently designed measuring cells of an electrokinetic analyzer. Acta chim. slovenica. 2010;57(3):700-6.

26.Thedsakhulwong A, Thowladda W. Removal of carbon contamination on silicon wafer surfaces by microwave oxygen plasma. J. Metals Mater. Min. 2008;18(2):137-41.

27. Ferrari AC, Robertson J. Interpretation of Raman spectra of disordered and amorphous carbon. Phys. Rev B. 2000 May 15;61(20):14095.

28. Ferrari AC, Robertson J. Raman spectroscopy of amorphous, nanostructured, diamond–like carbon, and nanodiamond. Phil. Trans. R. Soc. London A. 2004 Nov 15;362(1824):2477-512.

29. Papakonstantinou P, Zhao JF, Lemoine P, McAdams ET, McLaughlin JA. The effects of Si incorporation on the electrochemical and nanomechanical properties of DLC thin films. Diamond Related Mater. 2002 Mar 1;11(3-6):1074-80.

30. Nemanich RJ, Solin SA. First-and second-order Raman scattering from finite-size crystals of graphite. Phys. Rev. B. 1979 Jul 15;20(2):392.

31.Tuinstra F, Koenig JL. Raman spectrum of graphite. J. Chem. Phys. 1970 Aug 1;53(3):1126-30.

32. Shen AL, Weng YC, Chou TC. Effect of the analytic regions on the quality trend of diamond-like/graphitic carbon ratios in Raman Spectra. Zeitschrift für Naturforschung B. 2010 Jan 1;65(1):67-71.

33. Tai FC, Lee SC, Wei CH, Tyan SL. Correlation between ID⁄IG ratio from visible raman spectra and sp2/sp3 ratio from XPS spectra of annealed hydrogenated DLC film. Mater. Trans. 2006;47(7):1847-52.

34. Irmer G, Dorner-Reisel A. Micro-Raman studies on DLC coatings. Adv. Eng. Mater. 2005 Aug;7(8):694-705.

35. Yang KH, Joshi P, Rodenhausen KB, Sumant AV, Skoog SA, Narayan RJ. Correlation of zeta potential and contact angle of oxygen and fluorine terminated nitrogen incorporated ultrananocrystalline diamond (N-UNCD) thin films. Mater. Lett. 2021 Jul 15;295:129823.

36. Jaramillo-Cabanzo DF, Willing GA, Sunkara MK. Plasma etching chemistry for smoothening of ultrananocrystalline diamond films. ECS Solid State Lett. 2015 Aug 19;4(10):P80.

37. Ahmed MH, Byrne JA, Ahmed W. Characteristic of silicon doped diamond like carbon thin films on surface properties and human serum albumin adsorption. Diam. Relat. Mater. 2015 May 1;55:108-16.

38. Park YS, Son HG, Kim DH, Oh HG, Lee DS, Kim MH, Lim KM, Song KS. Microarray of neuroblastoma cells on the selectively functionalized nanocrystalline diamond thin film surface. Appl. Surf. Sci. 2016 Jan 15;361:269-76.

39. Klauser F, Hermann M, Steinmüller-Nethl D, Eiter O, Pasquarelli A, Bertel E, Seppi T, Lukas P, Lechleitner T. Direct and protein-mediated cell attachment on differently terminated nanocrystalline diamond. Chem. Vap. Depos. 2010 Mar;16(1-3):42-9.

40. Dalvi VH, Rossky PJ. Molecular origins of fluorocarbon hydrophobicity. Proc. Natl. Acad. Sci. U. S. A. 2010 Aug 3;107(31):13603-7.

41. V. Chakrapani, J. C. Angus, A. B. Anderson, S. D. Wolter, B. R. Stoner, and G. U. Sumanasekera, Science (80-.). 318, 1424 (2007).

42. Temmel S, Kern W, Luxbacher T. Zeta potential of photochemically modified polymer surfaces. In Characterization of Polymer Surfaces and Thin Films 2006 Jan 1 (pp. 54-61). Springer, Berlin, Heidelberg.

43. Kudin KN, Car R. Why are water− hydrophobic interfaces charged? J. Am. Chem. Soc. 2008 Mar 26;130(12):3915-9.

44. Barapatre A, Aadil KR, Jha H. Synergistic antibacterial and antibiofilm activity of silver nanoparticles biosynthesized by lignin-degrading fungus. Bioresour. Bioprocess. 2016 Dec;3(1):1-3.

45. Yoshijima Y, Murakami K, Kayama S, Liu D, Hirota K, Ichikawa T, Miyake Y. Effect of substrate surface hydrophobicity on the adherence of yeast and hyphal Candida. Mycoses. 2010 May;53(3):221-6.

46. Goswami RR, Pohare SD, Raut JS, Karuppayil SM. Cell surface hydrophobicity as a virulence factor in Candida albicans. Biosci. Biotechnol. Res. Asia. 2017 Dec 25;14(4):1503-11.

47. Zhao Q, Liu Y, Wang C, Wang S. Bacterial adhesion on silicon-doped diamond-like carbon films. Diamond Related Mater. 2007 Aug 1;16(8):1682-7.

48. Singleton DR, Masuoka J, Hazen KC. Surface hydrophobicity changes of two Candida albicans serotype B mnn4 Δ mutants. Eukaryot. Cell. 2005 Apr;4(4):639-48.

Captions

Figure 1. Schematic of the PECVD instrument utilized for Si-DLC deposition.

Figure 2. AFM images of (a) Si-DLC, (b) O-Si-DLC and (c) F-Si-DLC coatings.

Figure 3. Raman spectra of (a) Si-DLC, (b) O-Si-DLC, and (c) F-Si-DLC coatings.

Figure 4. XPS spectra of (a) Si-DLC, (b) O-Si-DLC and (c) F-Si-DLC coatings and deconvolution of (d) Si-DLC, (e) O-Si-DLC and (f) F-Si-DLC coatings in the C 1s region.

Figure 5. Water contact angle for (a) Si-DLC, (b) O-Si-DLC, (c) F-Si-DLC coatings and (d) zeta potential of Si-DLC, O-Si-DLC and F-Si-DLC coatings versus electrolyte solution pH value.

Figure 6. (a) Images of O-Si-DLC, F-Si-DLC, Si-DLC, and polystyrene (PS) with fungal pathogen *Candida albicans* after crystal violet staining. (b) Crystal violet quantification of *Candida albicans* on O-Si-DLC, F-Si-DLC, Si-DLC, and PS samples using absorbance measured at 600 nm. Four replicates of each sample were evaluated. Background absorbance of the control samples with the growth media without microorganisms were subtracted from the absorbance of each respective sample.

Table I. Atomic percentage of Si-DLC, O-Si-DLC, and F-Si-DLC

Table II Percentage of bonding contribution in C 1s

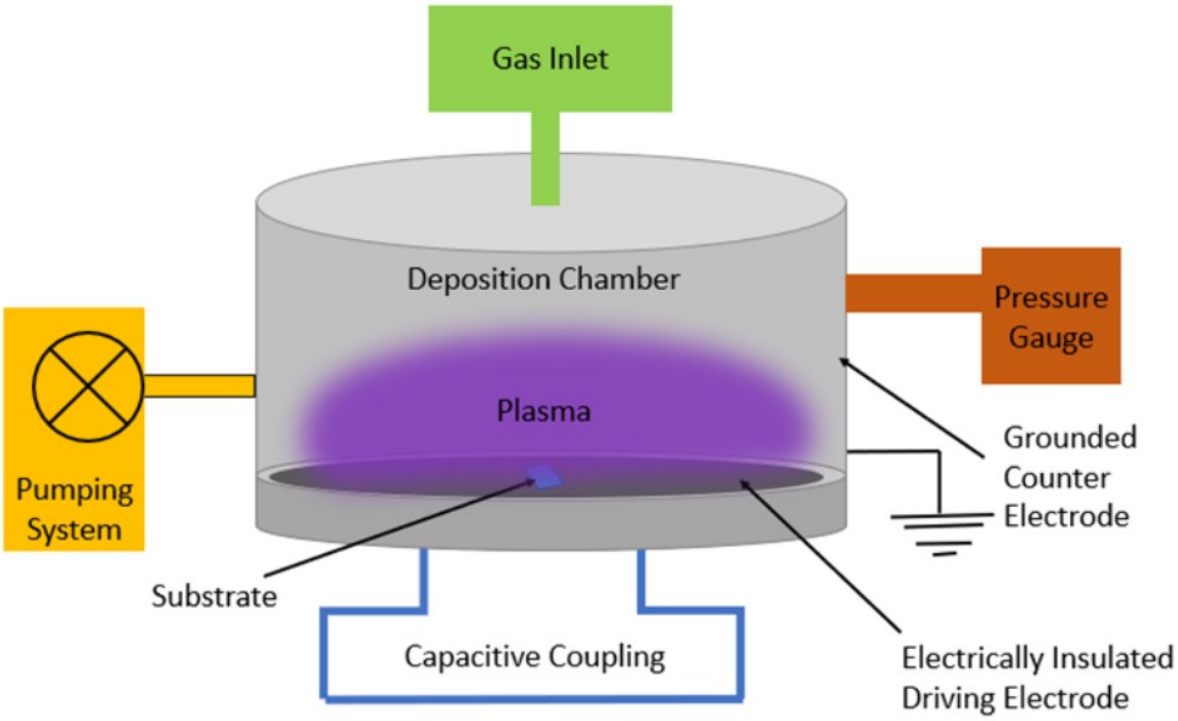

Figure 1. Schematic of the PECVD instrument utilized for Si-DLC deposition.

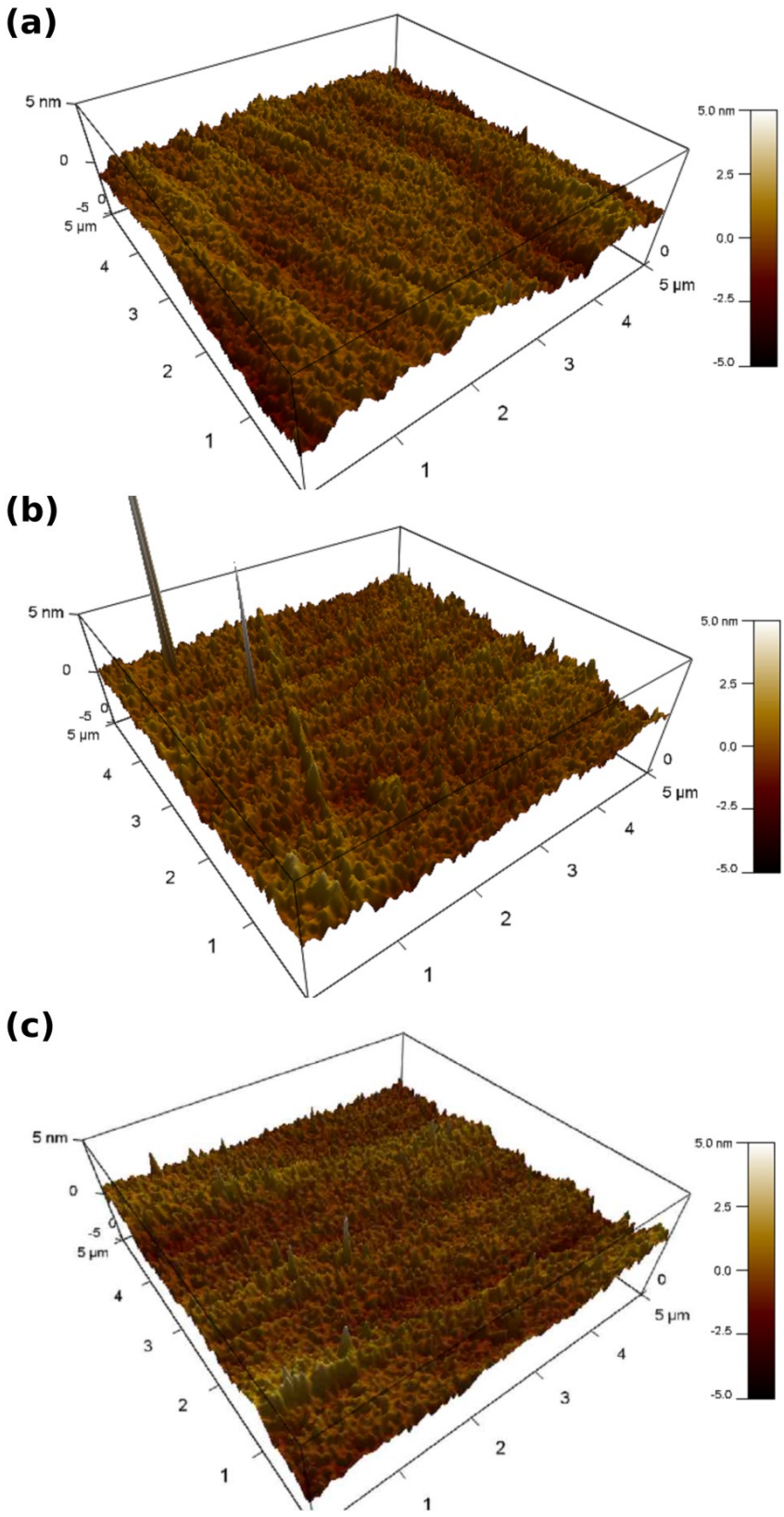

Figure 2. AFM images of (a) Si-DLC, (b) O-Si-DLC and (c) F-Si-DLC coatings.

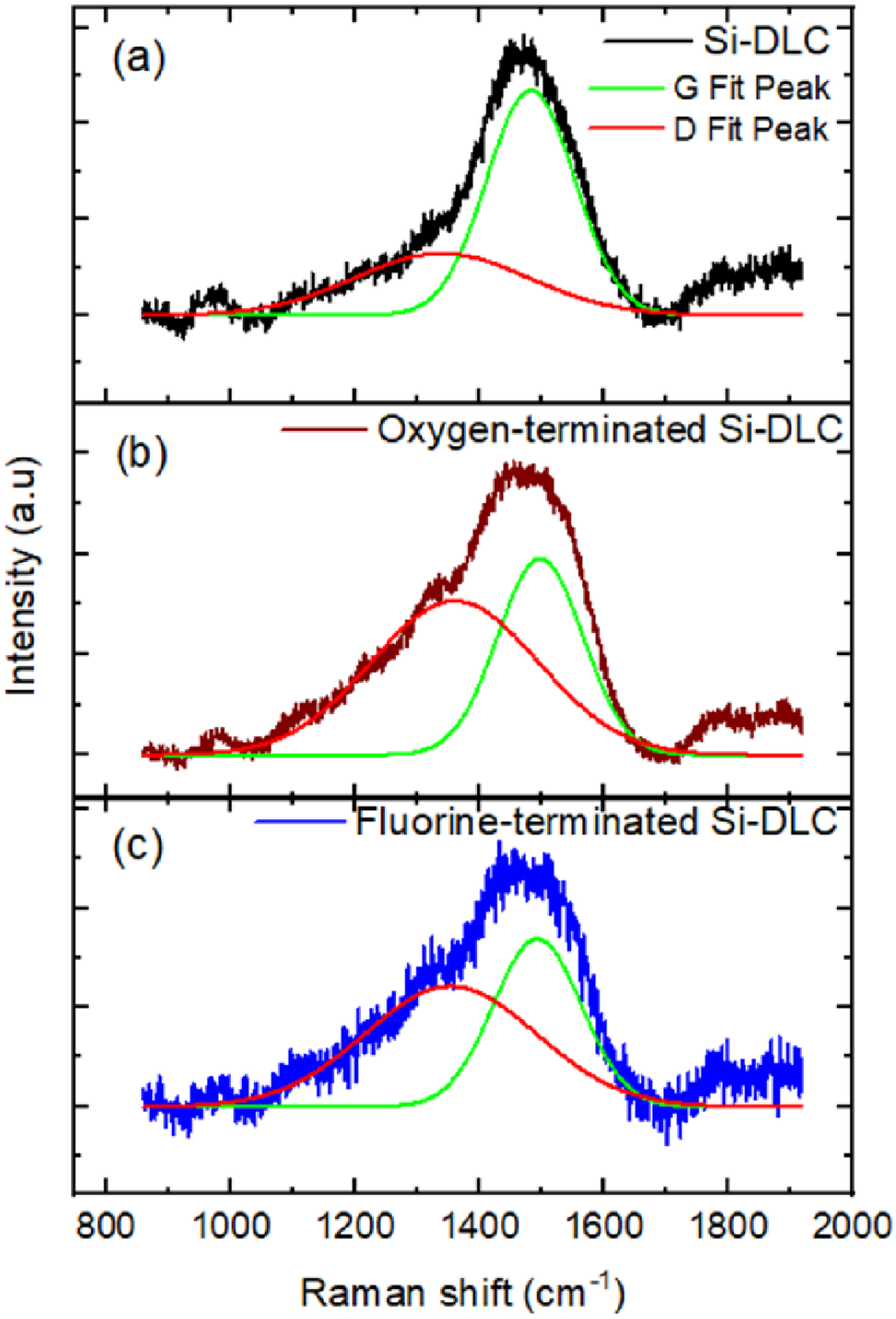

Figure 3. Raman spectra of (a) Si-DLC, (b) O-Si-DLC, and (c) F-Si-DLC coatings.

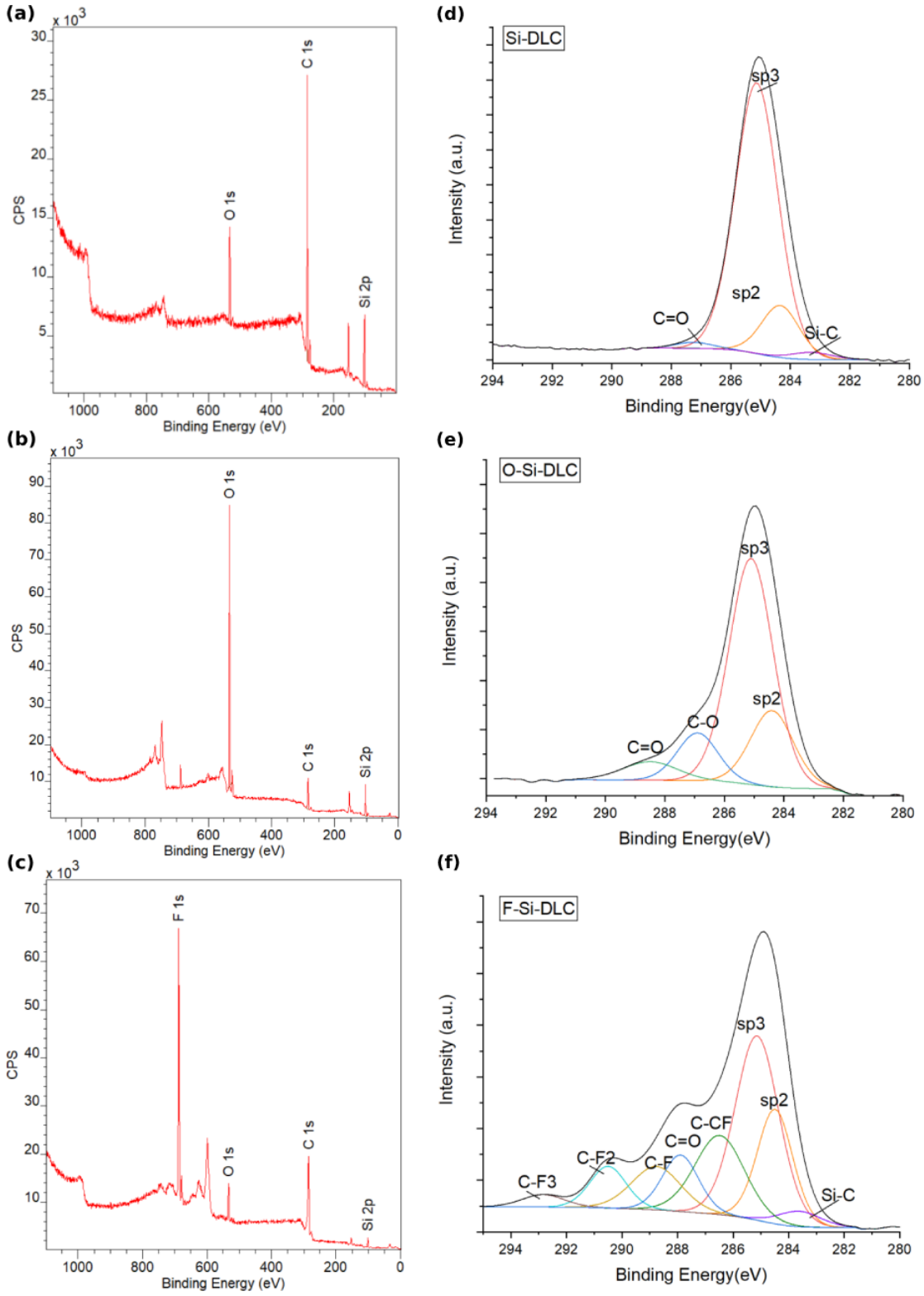

Figure 4. XPS spectra of (a) Si-DLC, (b) O-Si-DLC and (c) F-Si-DLC coatings and deconvolution of (d) Si-DLC, (e) O-Si-DLC and (f) F-Si-DLC coatings in the C 1s region.

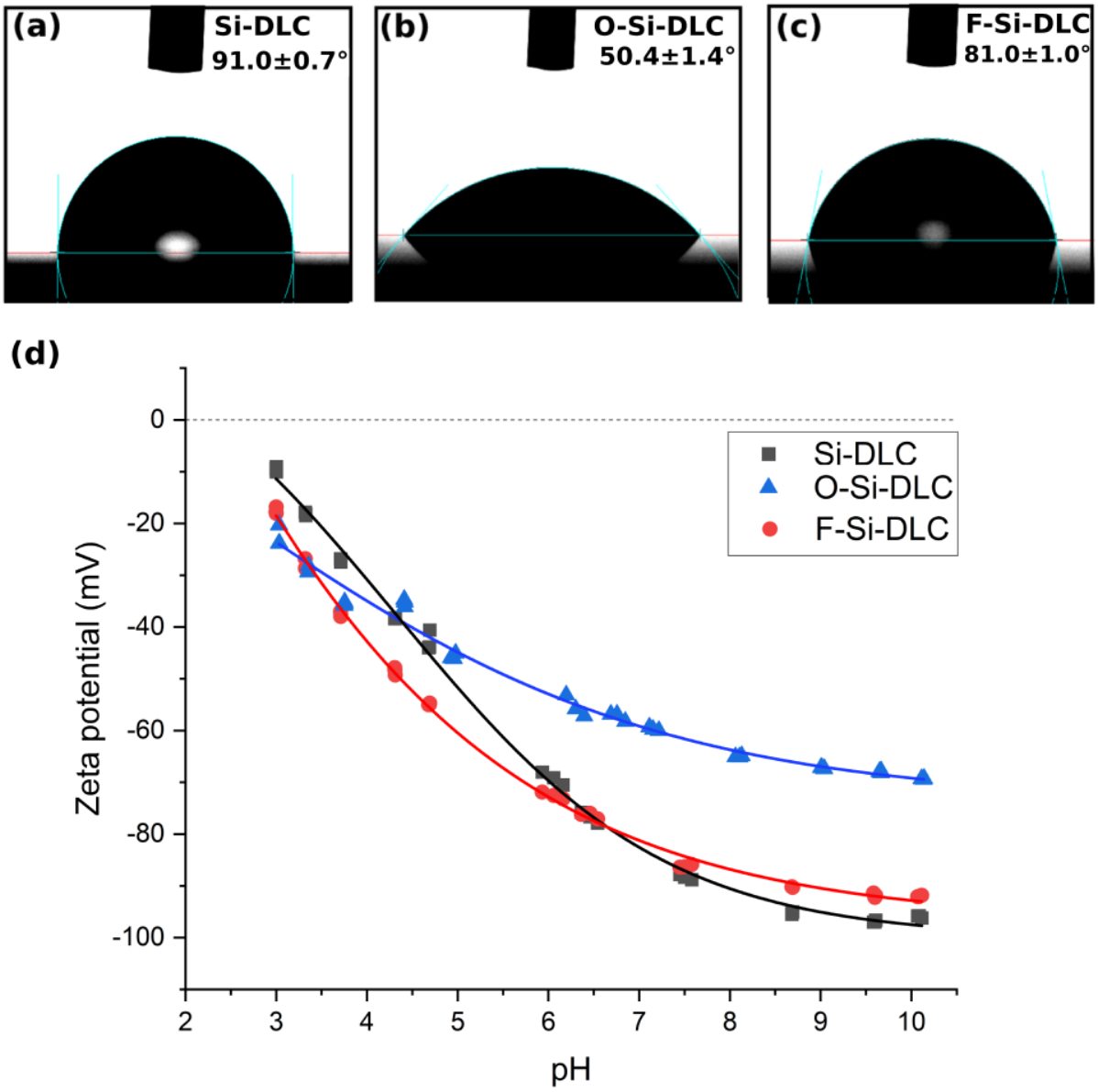

Figure 5. Water contact angle for (a) Si-DLC, (b) O-Si-DLC, (c) F-Si-DLC coatings and (d) zeta potential of Si-DLC, O-Si-DLC and F-Si-DLC coatings versus electrolyte solution pH value.

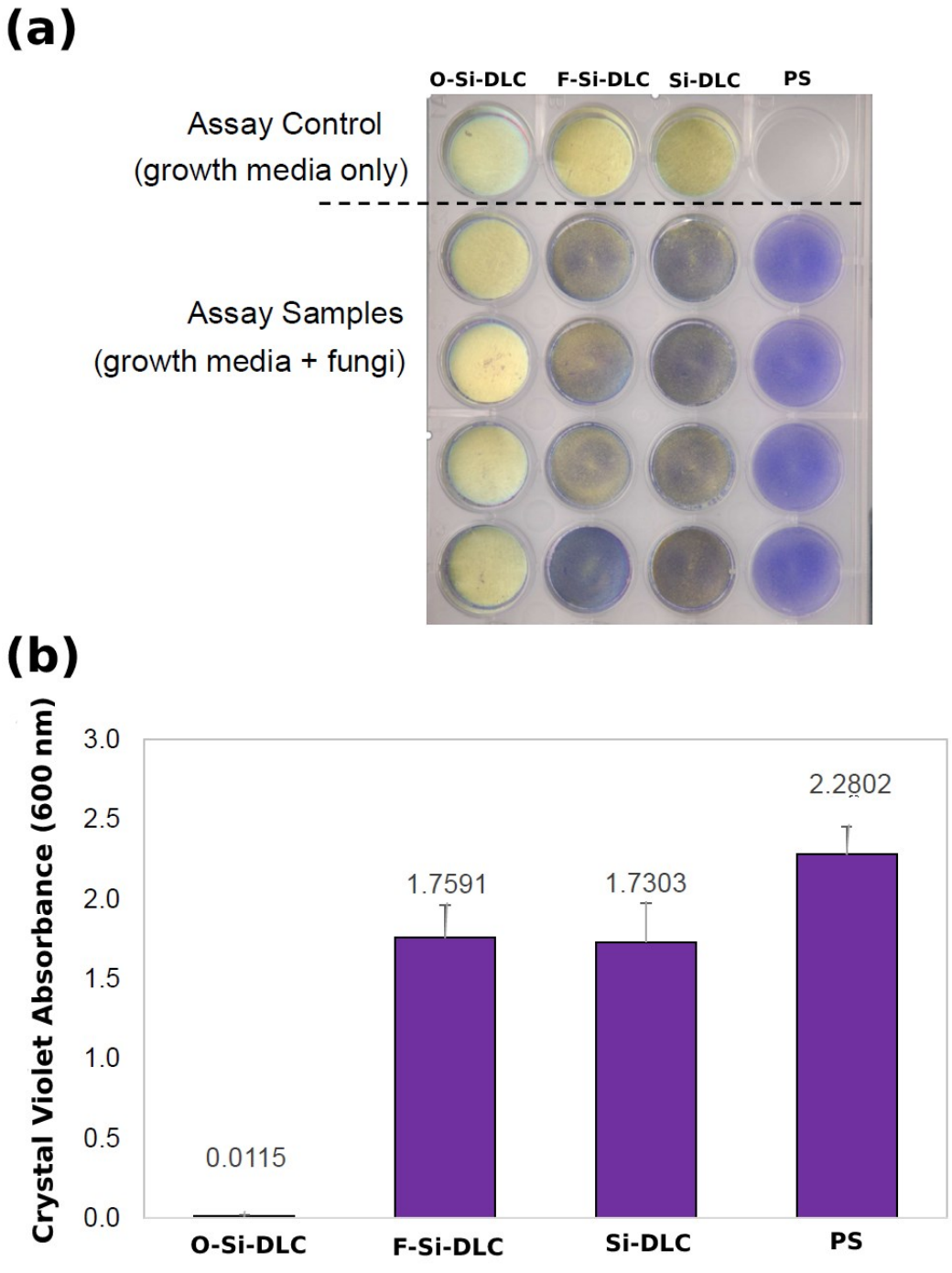

Figure 6. (a) Images of O-Si-DLC, F-Si-DLC, Si-DLC, and polystyrene (PS) with fungal pathogen *Candida albicans* after crystal violet staining. (b) Crystal violet quantification of *Candida albicans* on O-Si-DLC, F-Si-DLC, Si-DLC, and PS samples using absorbance measured at 600 nm. Four replicates of each sample were evaluated. Background absorbance of the control samples with the growth media without microorganisms were subtracted from the absorbance of each respective sample.

Table I. Atomic percentage of Si-DLC, O-Si-DLC, and F-Si-DLC

Sample	C	O	F	Si
Si-DLC	71	10	-	19
O-Si-DLC	23	54	-	23
F-Si-DLC	54	7	35	4

Table II Percentage of bonding contribution in C 1s

Sample	sp^2	sp^3	C-O	C=O	Si-C	C-CF	C-F	C-F2	C-F3
Si-DLC	14	82	-	2	2	-	-	-	-
O-Si-DLC	20	63	9	7	1	-	-	-	-
F-Si-DLC	18	35	-	9	3	17	9	7	2